3D neutronic analysis on compact fusion reactors: PHITS-OpenMC cross-comparison

Fusion Engineering and Design 202 (2024) 114323

Contents lists available at ScienceDirect

Fusion Engineering and Design

journal homepage: www.elsevier.com/locate/fusengdes

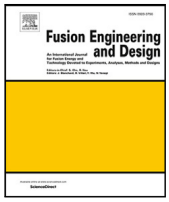

3D neutronic analysis on compact fusion reactors: PHITS-OpenMC cross-comparison

Federico Ledda [a,b,1], Davide Pettinari [c,1], Gabriele Ferrero [c], Zachary Hartwig [d], Francesco Laviano [a,b], Samuele Meschini [c], Simone Sparacio [a,b], Raffaella Testoni [c], Daniele Torsello [a,b,*], Antonio Trotta [e], Massimo Zucchetti [c]

[a] Department of Applied Science and Technology, Politecnico di Torino, Corso Duca degli Abruzzi 24, Torino, 10129, Italy
[b] Istituto Nazionale di Fisica Nucleare, Sezione di Torino, Via Pietro Giuria, 1, Torino, 10125, Italy
[c] Department of Energy, Politecnico di Torino, Corso Duca degli Abruzzi 24, Torino, 10129, Italy
[d] MIT Plasma Science and Fusion Center, 167 Albany St, Cambridge, MA, 02139, United States of America
[e] MAFE, Eni S.p.A., Via A. Pacinotti 4, Venezia, 30175, Italy

ARTICLE INFO

Keywords:
Compact fusion reactors
Monte Carlo
ARC
Neutronic analysis
PHITS
OpenMC

ABSTRACT

The development of high temperature superconducting tape technology enabled the design of compact fusion reactors, allowing faster development in the field. The reduced size makes even more important the evaluation of neutron flux on all components and at every region, including at the magnet position, to assess the lifetime of the materials and their performances during operations. Compactness, however, introduces new technological challenges, considering the reduced space available for shielding materials and the consequently harsher radiation environment for both structural and functional materials. Many different particle transport codes have been developed for nuclear engineering and fundamental physics purposes, each one relying on different algorithms and nuclear models, with different features and capabilities. In the present work the transport codes PHITS and OpenMC are compared, testing the impact on integral results such as the tritium breeding ratio and on spatially resolved neutron spectra of different nuclear libraries, nuclear models and codes, on a CAD imported 3D geometry of an ARC like fusion machine. The impact of different neutron source shapes is also investigated, from a simple ring-like source to a realistic toroidal plasma distribution, as well as the possibility of performing calculations on a 10° reduced domain, instead of on a full 360° geometry. The uncertainty introduced by each model and geometry choice is analyzed and the computational time required is briefly discussed.

1. Introduction

The recent developments in applied superconductivity, with the improved industrialization degree of High Temperature Superconducting (HTS) tapes [1,2], combined with the increasing interest in new technologies for decarbonization [3], gave a great impulse to research efforts in nuclear fusion, with both public and private investments [4]. While different designs are currently under investigation, D–T tokamaks seem to be the most promising option for the short term development of fusion power plants. The D–T reaction exploited in these tokamaks (D + T → ^{4}He (3.5 MeV) + n (14.1 MeV)) releases energy that is shared between alpha particles, confined by the magnetic fields of the tokamak, and neutrons, which free-stream through the magnetic fields and impact the structural materials surrounding the plasma. Since neutrons carry the largest fraction of the energy released by the D–T reaction (4/5 of the total) the computation and management of neutron fluxes, a classical issue also in fission technology, is confirmed to be essential in fusion engineering. Neutrons are indeed responsible for tritium breeding and heat deposition in the blanket, producing at the same time structural damages due to atomic displacement. Furthermore, the new road to compact reactors, made possible by the higher magnetic fields achievable with HTS, increased the centrality of neutronic analysis: while indeed smaller devices will show larger power density, lower cost and construction time [5], they will experience high nuclear fluences, especially from high energy neutrons [6,7].

The concept that compactness could lead to the design of cheaper fusion reactors was proposed in the Affordable Robust Compact (ARC) design [5], that is based on the use of demountable HTS magnets and

* Corresponding author at: Department of Applied Science and Technology, Politecnico di Torino, Corso Duca degli Abruzzi 24, Torino, 10129, Italy.
E-mail address: daniele.torsello@polito.it (D. Torsello).
[1] These two authors contributed equally.

https://doi.org/10.1016/j.fusengdes.2024.114323
Received 28 September 2023; Received in revised form 29 February 2024; Accepted 6 March 2024
Available online 19 March 2024

on the presence of a bulk liquid tank acting as breeding blanket and neutron shield. The reduced size of compact tokamaks limits the shielding capability of the blanket and the shielding itself, increasing the neutron flux impinging on delicate components, like HTS magnets [7]. The radiation environment will produce structural damage at a rapid pace, making it crucial to carefully estimate the radiation hardness of each material and component. As an example, a first estimate of the dpa expected for the HTS magnets for an ARC-like device after 10 years of irradiation is 0.52, an extreme condition for a ceramic material with functional purposes [7].

In this frame, Monte Carlo (MC) codes represent a fundamental tool to assess the effects of neutron irradiation by estimating the neutron flux distribution and spectra, and they have been exploited intensively in tokamak design and nuclear research. Tritium Breeding Ratio (TBR) optimization for compact devices [8], shielding calculations for safety design [9], preliminary heat exhaust management [10] are just some examples of well established applications in this field. Considering the centrality of such a tool, many different MC codes have been proposed [11–15] with many different purposes: from cross section evaluation to criticality calculations and to the radiation shielding design. These codes are built upon diverse physical models and algorithms, which introduce various approximations, and are optimized for different energy ranges. Moreover, MC codes are in general based on different nuclear libraries; these datasets can differ for the evaluated nuclides and they are affected by experimental uncertainties, so that cross sections can slightly differ from one to another. While the impact of different libraries has been evaluated for k-eigenvalue calculations, showing an agreement within 3σ [16], such a comparison has not been presented for a fusion application so far. Therefore, benchmarks and comparisons between codes can help the community in understanding general reliability of simulations and developers in improving the convergence of results.

In this paper the impact of two different MC codes (PHITS and OpenMC), of employed libraries, of geometrical approximations and of neutron source definition on the physically relevant neutronic parameters on a realistic design of the inner part of an ARC-like tokamak are evaluated. PHITS and OpenMC were chosen due to their suitable characteristics for studying the design of compact fusion reactors (such as the possibility to easily implement complex geometries, to modify the source code and to use parallelization schemes) and because a direct comparison between these two codes is lacking, despite both having been benchmarked against MCNP [17–19].

Another crucial aspect is the need to employ detailed geometrical models in MC simulations, since it has been shown that the differences on key results can be as high as 40% when using a simplified geometrical model instead of a realistic one [20]. The implementation of complex geometries however comes at the expense of a dramatic increase of computational costs, urging the need for an evaluation of how commonly employed simplification schemes affect neutronics results. Moreover, geometry declaration for complex and detailed elements is historically a big issue in transport codes, in which geometries are conventionally obtained by Boolean operations on primitive elements, like spheres, planes and cylinders. Such a procedure is clearly time consuming, prone to errors and not practical to rapidly deal with complex design modifications. The best approach to this issue is the employment of CAD files in MC codes, a possibility that has been recently introduced in several codes, although some difficulties still remain.

The declaration of the neutron source is another element of complexity in MC simulations; while simple shapes are available by default in all the codes, a more refined solution for plasma emission is in general not included. Simple rings have been exploited for this purpose in the past [21] and equations for implementing custom plasma sources have been proposed [22], but the differences introduced by these kinds of solutions have not been quantified.

Overall, by focusing on these aspects, this study is instrumental in expanding the possibility to introduce MC codes in multi-code CAD-based workflows for the design and optimization of compact fusion reactors.

2. Methods

2.1. Monte Carlo codes

In the present work a comparison between the code PHITS (version 3.30) and OpenMC (version 0.13.3) is carried out for nuclear fusion applications. PHITS is a multiplatform, multipurpose FORTRAN-based MC code proposed by the Japanese Atomic Energy Agency JAEA, able to transport and collide nearly all particles (neutrons, ions, electrons, photons, positrons, hadrons, etc.), over a large energy range (10^{-4} eV to TeV). It has been used for accelerator design, radiation therapy and many other applications, excluding criticality calculations. It allows the import of CAD based geometries using a tetrahedral mesh to reproduce complex domains, and supports MPI, OpenMP, and hybrid parallelization schemes. The native nuclear data library used in PHITS is JENDL-4.0 in the ACE format (but any nuclear data library in such a format can be chosen) [12], while different physical models are available for neutrons with energies higher than 20 MeV. The PHITS code is also equipped with an *ad-hoc* sampling method of secondary particles using nuclear data libraries, the Event Generator Mode [23]. PHITS was validated against MCNP [17,18,24–26], GEANT4 [24–26], FLUKA [24,27] and other codes [27], and previous attempts to use PHITS in tokamak neutron calculations have been performed in Japan, for shielding purposes [9,28].

OpenMC is a community-developed MC code, originally proposed by the computational reactor physics group of the MIT [29]. It is written in C++, and it has a user-friendly Python API that leverages on common Python packages for pre-processing and post-processing. All version control of OpenMC and its documentation are handled through the git-distributed revision control system, and the code is available on GitHub. It implements neutron and photon transport, being particularly devoted to fission reactor applications, like k-eigenvalue or subcritical multiplication calculations. It supports both Computational Solid Geometry (CSG) and CAD imported geometries [30], relying for the latter on the Direct Accelerated Geometry Monte Carlo (DAGMC) software [31], parallelization and both continuous and multigroup transport. The parallelization is enabled by a hybrid MPI and OpenMP programming model. The continuous-energy particle interaction data is based on the HDF5 format that can be generated from ACE or ENDF files produced by NJOY. OpenMC has been applied to many different designs, like PWR [32], IAEA benchmark Material Test Reactor [33], MSR [34] and tokamaks [35]. It was also validated against MCNP on an ARC-class tokamak [19].

Overall, PHITS and OpenMC have different characteristics and potentialities, both were benchmarked against MCNP, and each can be suitable for fusion technology applications. However, to the best of our knowledge, no direct cross-comparison on fusion topics between these two codes, fully exploiting their handling of complex 3D geometries and parallelization schemes, has been published.

2.2. Geometry and CAD import

In the present work, neutronic simulations are performed on a model of an ARC-like tokamak vacuum vessel (VV) and liquid immersion blanket (LIB). The model consists in a D-shape plasma chamber, surrounded by a tungsten first wall (FW), an Inconel 718 VV submerged in a FLiBe tank [5,10,35]. In particular, the model is composed by seven layers as summarized in Table 1, three of which are Inconel structural layers indicated in the text and figures as STR1, STR2 and STR3. Tungsten is employed as first wall material, to face the plasma. The presence of Be in the fourth layer is justified by the need for neutron multiplication to reach the desired TBR, while FLiBe performs the function of tritium breeder and tritium carrier. Moreover, FLiBe is exploited also as coolant and radiation shield. The geometry considered in the present paper for an ARC-like tokamak reproduced that proposed

Table 1
Thickness and total volume of each layer in the geometry definition of the model. The thickness here reported is evaluated at the outboard mid plane. Note that for the FLiBe in the tank it changes as shown in Fig. 1.

Material	Component	Thickness (mm)	Volume (m^3)
Tungsten	First wall	1	0.35
Inconel-718	VV inner structural material (STR1)	10	3.53
FLiBe	Coolant channel	20	7.10
Beryllium	Neutron multiplier	10	3.57
Inconel-718	VV outer structural material (STR2)	30	10.81
FLiBe	Coolant tank	1000	350.17
Inconel-718	Tank wall (STR3)	20	14.00

Table 2
Plasma parameters from [5] used for the definition of the plasma source in PHITS and OpenMC.

Parameter	Variable	Value	Units
Major radius	R_0	3.3	m
Plasma semi-minor radius	a	1.13	m
Plasma elongation	κ	1.84	–
On-axis temperature	T_0	27	keV
On-axis density	n_0	$1.8 \cdot 10^{20}$	m^{-3}
Shafranov factor	–	0.44	–
Helicity	e	1.557	–
Triangularity	d	0.27	–

in [10,19], both in the shape and for what concern the different layers thickness.

A detailed 3D CAD model was built by the authors in SolidWorks®, its poloidal cross section is shown in Fig. 1, while the components and materials are summarized in Table 1 and in the supplementary material [7]. The CAD model employed here was imported in PHITS using its native function for dealing with tetrahedral-mesh geometries [36] (generated using COMSOL® in our case), and via the DAGMC tool in OpenMC, employing the package *stl-to-h5m* [31,37]. This latter package generates *h5m* files complete with materials tags and ready for OpenMC calculations, but does not perform imprinting or merging of the geometry. Since for a DAGMC-based analysis to function optimally all surfaces must be imprinted and merged, and having chosen this conversion method, our geometry was joined directly in SolidWorks. Conversion systems that perform directly imprinting and merging could result in fast simulation times in DAGMC-enabled codes.

Simulations were performed both on a complete 360° axisymmetric reactor geometry and on a reduced 10° domain, to state the differences in terms of computational time, error reduction and compatibility of the obtained results. Reflective boundary conditions (BC) have been set to reproduce the full geometry in the reduced domain. No ports, penetrations or other refined structures of the design have been included at this stage.

2.3. Source geometry

Being the simulations devoted to tokamak machines, a neutron source reproducing the shape of a fusion plasma has been used; while such a source is readily available in OpenMC [38], it has been coded expressly for PHITS as a user-defined source, based on the same reference of the OpenMC one [22]. The neutron source has a toroidal distribution, with temperature and density depending on the radial and axial coordinates, and can be used to reproduce both H and L confinement modes. All the main plasma parameters, such as Shafranov factor and helicity, are taken into account and the values used in the present simulations are listed in Table 2. Temperature and density

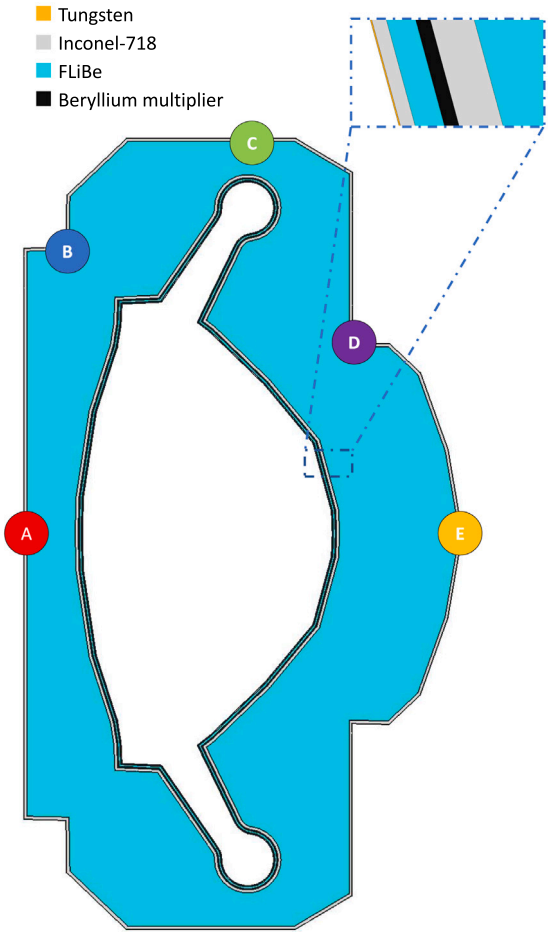

Fig. 1. 2D sketch of an ARC-class VV and LIB. Each layer is depicted with a different color. Table 1 reports the thickness of each layer. Five key points analyzed throughout this work are depicted on the outer tank wall.

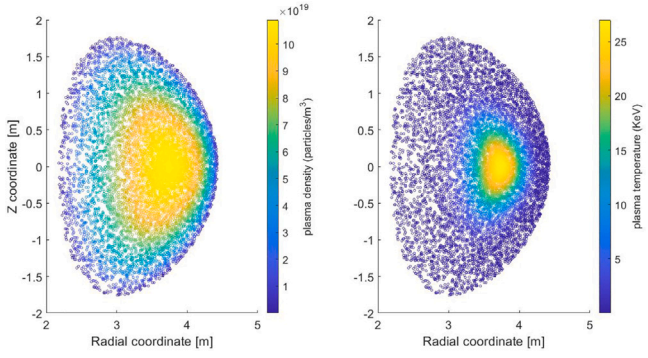

Fig. 2. Source density and temperature.

distribution of the source are shown in Fig. 2. The emissivity of the source was evaluated on the basis of the plasma power [5] in 1.8×10^{20} n/s.

2.4. Nuclear data libraries

Nuclear data libraries are fundamental for MC calculations, therefore the present work offers a comparison between two different codes using the same libraries and a test on each code itself when running with different libraries. The chosen libraries are the JENDL-4.0 [39], proposed as the Japanese standard libraries for both fission reactors,

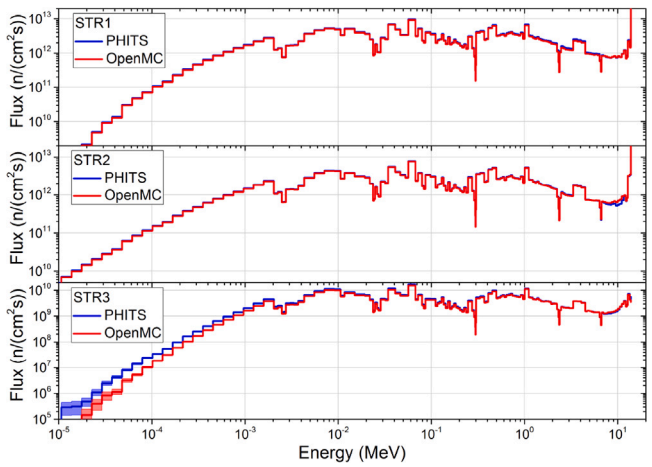

Fig. 3. Neutron spectra on the three structural layers calculated on the full 360° geometry with the PHITS (blue lines) and OpenMC (red lines) codes. Shaded areas represent the absolute error on the simulation.

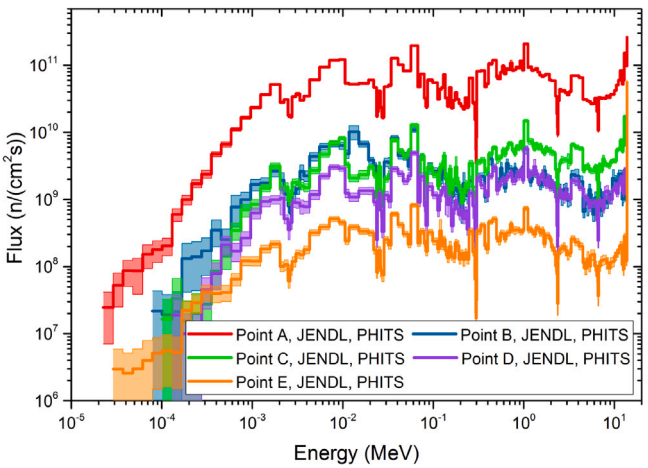

Fig. 4. Neutron spectra at different locations on STR3, the color legend is the same of Fig. 1. Shaded areas represent the absolute error on the simulation. Point A is the one with the harshest radiation environment.

fusion neutronics and shielding calculations, the ENDF/B-VIII.0, a well-established dataset under development since 1968 and the default library for codes like MCNP and GEANT4 [40,41] and FENDL-3.2, a nuclear library for fusion application, developed in the frame of the international effort coordinated by the IAEA Nuclear Data Section [42]. JENDL-4.0 includes 406 nuclides, with incident neutrons energy between 10^{-5} eV to 20 MeV, while the ENDF/B-VIII.0 contains data for 163 nuclides, most of them up to 140 MeV [41]. FENDL-3.2 includes 180 materials [42].

As introduced above, the use of different datasets can bring to discrepancies in results. The number and species of nuclides evaluated and the processing procedure for the generation of MC-readable cross section libraries can be responsible for partial inconsistencies. Moreover, different codes might interpolate between data of the same library with different methods, so the data-density of each library can be another relevant parameter. The benchmark between the two codes is performed comparing integral fusion-relevant parameters, such as the TBR and the volumetric power deposition, and neutron spectra, evaluated with the energy group structure *vitamin-j 175*.

3. Results and discussion

This section shows the impact of different modeling approaches and choice of nuclear data libraries on the neutronic analysis. Section 3.1 focuses on the comparison of spectra obtained with the two MC codes, while 3.2 on the variations of the spectra along the poloidal angle. Section 3.3 compares the results obtained with the reduced geometry (10° slice of the reactor with reflective BC) and with the complete geometry. Section 3.4 shows the results for a simple ring source and a customized plasma source as defined in [38]. Section 3.5 compares the results obtained with the ENDF/B-VIII.0, JENDL-4.0 and FENDL-3.2 libraries. Finally, in Section 3.6 computational costs are presented.

3.1. Code results comparison

We start by considering the neutron spectra computed by the two codes on the Inconel 718 layers for the full model as shown in Fig. 3; the calculations have been performed using ENDF/B-VIII.0 library and about 10^9 source neutrons divided into 240 batches, without variance reduction schemes. As can be noted, the large amount of simulated particles produces relative errors well below the reference value of 10%, a threshold often considered reasonable when comparing MC results [43]. The attenuation of the neutrons across the reactor is responsible for the different spectra shown by the different layers (shown in the three panels). The two codes provide very comparable results on the first two structural layers, whereas the third structural layer, the farthest from the source, presents some discrepancies. It is worth noticing that also in this case the particular characteristics of the two curves appear to be compatible, and the variation in the absolute values becomes significant only below about 1 keV.

3.2. Neutron spectra dependence on poloidal position

It is worth to notice that the results discussed above have been computed tallying the spectrum over the complete region, but sensible differences can be found with a more detailed analysis. For example, the VV shielding thickness differs between the inboard and the outboard, so that the inner board is more loaded from a neutronic point of view, resulting as a more critical position for radiation damage.

This can be evaluated in detail by studying the 5 points at different poloidal positions indicated in Fig. 1, for which the neutron spectra are reported in Fig. 4 for PHITS. The JENDL library was used since it is the native library for PHITS. Results are not shown for OpenMC because it does not allow to tally small, manually-defined regions over CAD imported geometries. As can be seen, the most loaded region is at the inboard midplane, whereas the outboard midplane has a lower flux. It should be noted that when the spectra is evaluated over the whole region, the obtained values are basically an average between these two extremes. Despite the simulation involved again more than 10^9 particles, the absolute error is larger than tallying on the full region, due to the smaller size of the detector. However, on the relevant part of the spectrum the relative error for the point A is always in the acceptance region. Being at the interface with the magnet system, points A gives an indication of the regions in the TF magnets in which radiation damage on the HTS tape would have a stronger impact, and where shielding design should focus.

3.3. Geometry simplification

In this section, the effect of geometrical approximations on neutron spectra, TBR and heat deposition of the reduction of the domain is investigated. The reason for this benchmark lies in the fact that as long as the device is symmetrical, i.e. for simplified calculations, in which the presence of penetration or instrumentation is neglected, the usage of reflective BC can allow an increase of the spatial resolution, reducing the mesh dimensions and hence relaxing the memory requirements. However one should be sure that this approximation does not influence the results.

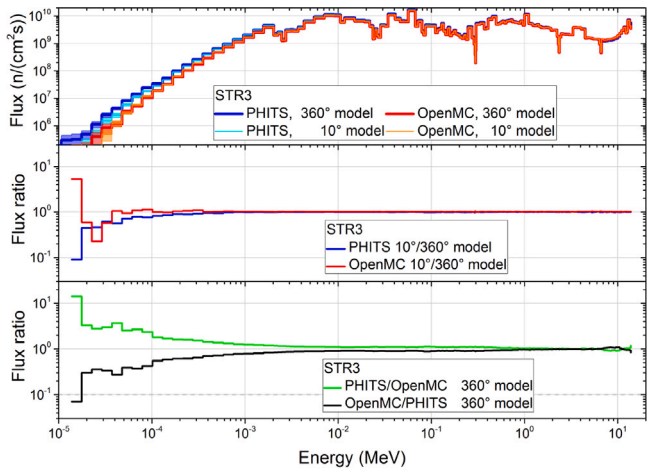

Fig. 5. Panel 1: comparison of the neutron spectra on the outer structural layer STR3 in the 10° model with reflective BC (light colors) vs. the full 360° model (dark colors), with PHITS (blue shades) and OpenMC (red shades). Panel 2: ratios of the neutron spectra obtained with the 10° to the spectra from the 360° model, computed with the two codes. Panel 3: ratios of the neutron spectra computed with PHITS and OpenMC on the 360° model.

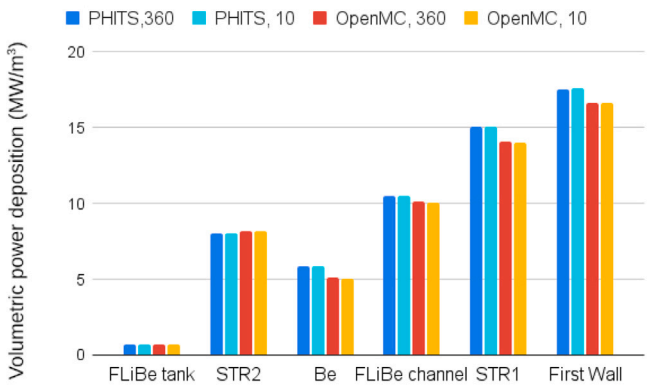

Fig. 6. Volumetric power deposition: reduced vs. full domain in PHITS and OpenMC evaluated with the ENDF/B-VIII.0.

To highlight the difference between complete geometry and the 10° model with reflective BC, neutron spectra on the external Inconel 718 layer (*i.e.* the case with the worst agreement between MC codes reported in Fig. 3) have been examined in Fig. 5. The second and third panels of Fig. 5 show the ratio between the fluxes presented in the first panel: a divergence from the value of 1 indicates a non-ideal agreement. The second panel shows differences arising from the geometry reduction, whereas the third focuses on the MC code choice. Both code and geometry reduction choices have a negligible effect above 1 keV, below this value the chosen MC code starts to play a role, whereas the effect of geometry reduction emerges only below about 100 eV.

The effects of the geometrical model have also been tested on the deposited power on the VV regions and on TBR. Considering the power deposition, shown in Fig. 6, we find a perfect agreement between reduced and full domain outputs within a code, and only a 5%–15% difference between OpenMC and PHITS, the maximum difference being on the Be multiplying layer. As an example, the deposited volumetric power on the FW computed with PHITS is higher than the one provided by OpenMC by 0.99 MW/m^3. Generally, we found a good agreement also with other published works [10,19,44], although the used geometry and models are slightly different (see Supplementary material [45] for details).

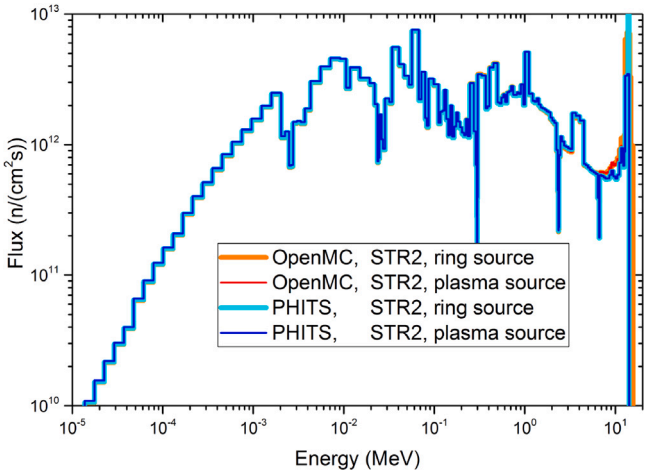

Fig. 7. Neutron spectra calculated on the second structural layer with the simple ring source (thicker, lighter lines) vs. realistic plasma source (thinner, darker lines) with PHITS (blue shades) and OpenMC (red shades).

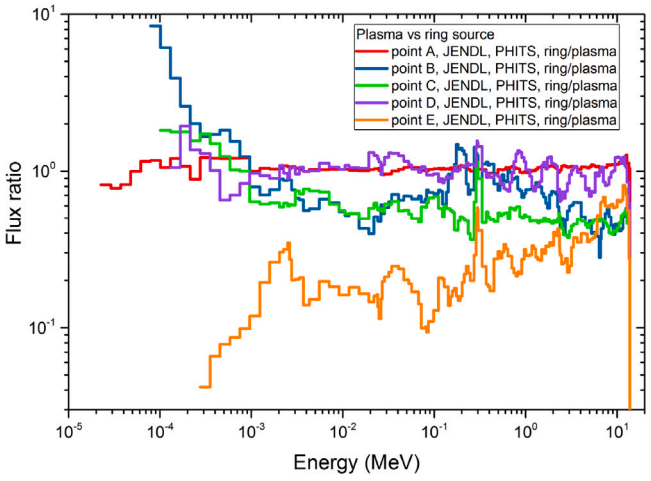

Fig. 8. Flux ratios between the neutron spectra evaluated with PHITS using the simple ring and using the plasma source for point A, B, C, D and E. Curves were smoothed for clarity of presentation, ras data is shown in the Supplementary Material [45].

The TBR (values summarized in Table 3) shows a relative difference between the two codes in the range 1%–2%, with a negligible effect of the considered domain. The TBR computed by OpenMC is slightly lower than that computed by PHITS for both the 10° and 360° models. The effect of the choice of library on the TBR will be discussed in Section 3.5.

3.4. Source simplification

In this section, the realistic plasma sources are compared with a simple ring source emitting fusion neutrons. The radius of the ring has been set equal to the major radius presented in Table 2.

Averaging the neutron spectra on a region cancels the effect of geometrical complexity in the source, as confirmed in Fig. 7. This is easily understandable, considering that both the sources are completely enclosed in the regions used as detectors, so that all the emitted neutrons are caught. Conversely, measuring the neutron spectrum on smaller regions at different poloidal positions allows differences to emerge, as presented in Fig. 8. Here results are presented in terms of flux ratios between the data obtained with the ring source and with the plasma source.

Table 3
TBR values computed with the two MC codes for the different geometries and libraries considered.

Code	Geometry	Library	TBR value ± uncertainty (1 σ)
PHITS	full domain	ENDF/B-VIII.0	1.0766 ± 0.0001
PHITS	full domain	JENDL-4.0	1.0736 ± 0.0001
PHITS	full domain	FENDL-3.2	1.0703 ± 0.0001
PHITS	10° domain + reflective BC	ENDF/B-VIII.0	1.0761 ± 0.0001
OpenMC	full domain	ENDF/B-VIII.0	1.0626 ± 0.0001
OpenMC	full domain	JENDL-4.0	1.0737 ± 0.0001
OpenMC	full domain	FENDL-3.2	1.0495 ± 0.0001
OpenMC	10° domain + reflective BC	ENDF/B-VIII.0	1.0625 ± 0.0001

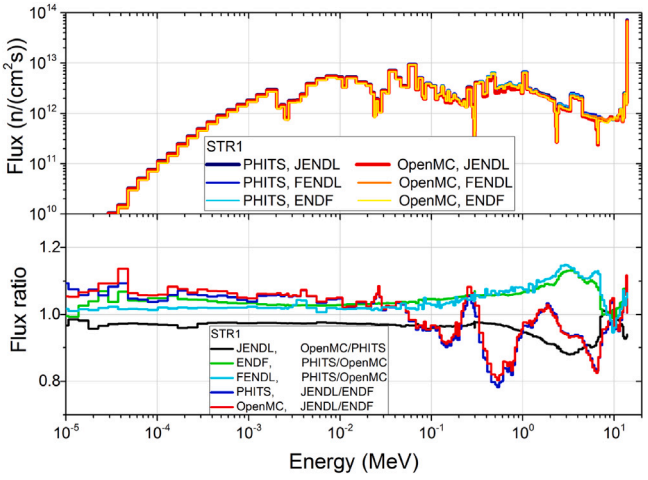

Fig. 9. Upper panel: neutron spectra on the first Inconel layer calculated on the reduced domain using the libraries JENDL-4.0, FENDL-3.2 and ENDF/B-VIII.0 and the codes PHITS (blue shades) and OpenMC (red shades). Lower panel: representative selection of the flux ratios between the spectra presented in the upper panel. Differences between the two codes with the JENDL-4.0 library (black curve), ENDF/B-VIII.0 (green curve), and FENDL-3.2 (cyan curve) and between the native libraries of the two codes within the same code (blue for PHITS and red for OpenMC).

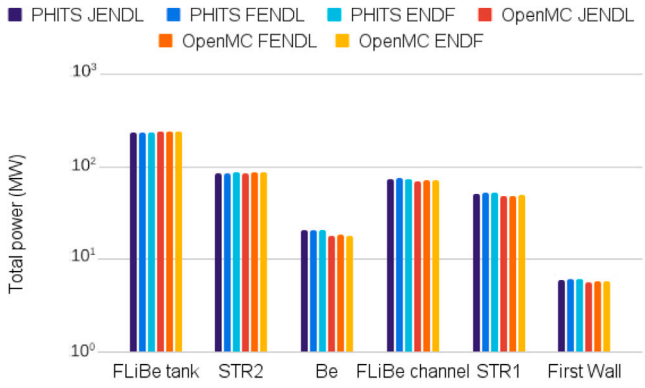

Fig. 10. Total power deposition in each region, for each nuclear data library (JENDL 4.0, FENDL 3.2, ENDF/B-VIII).

The spectrum at point A, coincident with the inboard region, is weakly affected by the source employed, due to its low shielding thickness, high symmetry position, and vicinity to the center of the chamber. The larger effect interests points B, C, D and E due to geometrical reasons.

3.5. Library comparison

The effects of different nuclear libraries on neutron spectra, TBR and power deposition have been tested running the same calculation with 3 different data structures, ENDF/B-VIII.0 [40], JENDL-4.0 [39] and FENDL-3.2 [42], on the same domain. The first structural layer has been chosen to perform this benchmark because of its lower relative errors. The simulations were run on the reduced domain and results in term of neutron spectra are shown in Fig. 9.

Also in this case, to state in a more proper manner results compatibility, flux ratios have been computed and shown in the subplot of Fig. 9. The choice of nuclear data appears to have a larger impact than the domain reduction: for low energies, the relative difference is below 10%, while above 1 keV is as high as 20%.

On the other hand, the good agreement in the power deposition presented in Fig. 6, is found with all the evaluated nuclear data libraries, as shown in Fig. 10. Within the same code, power deposition estimates vary by less than 4% when changing nuclear data library. Literature data are summarized in Table 4, a good agreement is found for all layers except for the first wall, where we note that literature data is much more scattered and affected by simulations choices.

For what concerns TBR, neither the effect of the usage of a different code nor of a different library seems to be prevalent, as explicated in Table 3. The TBR computed by OpenMC is lower for all the nuclear data libraries but the JENDL-4.0, for which results are in good agreement with PHITS. The largest discrepancy is found for the FENDL-3.2. It should be noted that both the JENDL-4.0 and the FENDL-3.2 are not official OpenMC libraries, but they have been processed from ACE by the authors with the help of available scripts [46,47]. Despite being of the order of few percents, the differences between the two codes are far above the one reported by Bae et al. [19] between MCNP and OpenMC (1.05382 ± 0.00021 for MCNP - 1.05367 ± 0.00014 for OpenMC). Slightly higher TBR estimates are reported using MCNP (1.080 [10]) and Serpent 2 (1.085 [44]).

3.6. Computational cost

All the simulations were performed with 10^9 source particles on 5 nodes of HPC4 [48], with the Intel compiled MPI version of PHITS and OpenMPI implemented in OpenMC. Each node of the cluster has two CPUs AMD EPYC 7402 24-Core Processor, for a total of 240 cores. It must be considered that for MPI run in PHITS, one thread must be reserved for mastering the processes, so that the effective MPI threads were 239.

The average effective running times for the proposed simulation, have been of about 3 h and 3 h and 50 min (for the reduced and complete domain, respectively) in PHITS, while the simulations in OpenMC required about 5 h and 30 min and 12 h and 40 min, respectively, for the same two domains. No appreciable differences in the running times were introduced by using different nuclear libraries (see the Supplementary Material for details, slight variations are due to performance fluctuations of HPC4).

Moreover, it should be considered that the number of mesh elements in PHITS is about $1. \times 10^6$ and 1.3×10^7 for the reduced and complete domains, respectively, and about 5.5×10^4 and 2×10^6 in OpenMC (the smaller number of elements in OpenMC is imposed by the use of the package *stl-to-h5m* [37]).

The above considerations proved that the use of the reduced domain with reflective BC is a valid simplification scheme, allowing not only a

Table 4
Total power deposition (MW) in each VV and blanket components from previous works. The ENDF/B-VII.1 was used in [19], the ENDF/B-VIII.0 was used in [44], while in [10] the nuclear data library used is not reported. STR3 is not present because it was not computed in the references.

Component	Kuang et al. (MCNP) [10]	Bae et al. (MCNP - OpenMC) [19]	Aimetta et al. (Serpent 2) [44]
First wall	8.4	8.16 - 7.96	7.41
STR1	39.6	36.29 - 35.59	35.66
FLiBe in VV channel	77.7	73.29 - 72.39	79.09
Beryllium	22.4	21.78 - 21.51	21.60
STR2	78.9	76.03 - 75.22	73.33
FLiBe in tank	255	251.99 - 252.84	255.02
Total	482	467.54 - 465.50	475.92

reduction on the size of mesh files (by a factor of 13 in PHITS and of 33 in OpenMC), but also a reduction in the running time, preserving the precision of the results.

Finally, PHITS appears to be more efficient in dealing with transport calculation on finely meshed geometries, being faster despite the much higher number of employed elements.

4. Conclusions

In this paper, we compared the OpenMC and PHITS MC codes for fusion applications, working on a 3D CAD-based geometry of the ARC design. CAD import was successfully implemented and the simulations were performed with parallelization schemes on a supercomputer, allowing the investigation of large and complex geometries in reasonable computational times. We find that geometry reduction through the imposition of suitable BC on the simulation is a valid method to reduce the size of the geometry without affecting the results. On the other hand, the simplification of the particle source might lead to a bad evaluation of local particle spectra, while leaving integral results unaffected. The choice of the MC code and of the nuclear library has a non negligible effect on the calculated TBR (values ranging from 1.0495 to 1.0766), while neutron spectra and deposited power yield a satisfying agreement in all cases. PHITS allowed a finer geometrical control over the evaluated quantities and proved to be faster than OpenMC. Overall, OpenMC and PHITS are found to yield comparable results in the neutron analysis of CAD-based models of fusion reactors, with reasonable computational times if parallelization schemes are used.

CRediT authorship contribution statement

Federico Ledda: Investigation, Software, Formal analysis, Data curation, Writing – original draft. **Davide Pettinari:** Investigation, Software, Formal analysis, Data curation, Writing – original draft. **Gabriele Ferrero:** Resources. **Zachary Hartwig:** Supervision, Validation, Writing – reviewing & editing. **Francesco Laviano:** Writing – reviewing & editing, Supervision, Validation, Project administration, Funding acquisition. **Samuele Meschini:** Methodology, Data curation, Formal analysis, Writing – original draft. **Simone Sparacio:** Resources, Investigation, Data curation. **Raffaella Testoni:** Supervision, Writing – reviewing & editing, Funding acquisition. **Daniele Torsello:** Conceptualization, Methodology, Data curation, Writing – original draft, Supervision, Funding acquisition. **Antonio Trotta:** Supervision, Project administration, Funding acquisition. **Massimo Zucchetti:** Supervision, Validation, Funding acquisition.

Declaration of competing interest

The authors declare the following financial interests/personal relationships which may be considered as potential competing interests: Daniele Torsello reports financial support was provided by Eni SpA. Federico Ledda, Simone Sparacio, Davide Pettinari, Samuele Meschini report financial support was provided by Eni SpA. Francesco Laviano, Massimo Zucchetti, Raffaella Testoni report a relationship with Eni SpA that includes: funding grants.

Data availability

Data will be made available on request.

Acknowledgments

This work is partially supported by the Ministry of Education, Universities and Research through the National Recovery and Resilience Plan funded by the European Union-NextGenerationEU, by the European Cooperation in Science and Technology (COST) action CA19108: “High-Temperature Superconductivity for Accelerating the Energy Transition”, by the Italian Ministry of Foreign Affairs and International Cooperation, grant number US23GR16, and by Eni S.p.A. Support from CINECA for high-performance computing is also acknowledged. D.T. also acknowledges that this study was carried out within the Ministerial Decree no. 1062/2021 and received funding from the FSE REACT-EU - PON Ricerca e Innovazione 2014–2020. This manuscript reflects only the authors’ views and opinions, neither the European Union nor the European Commission can be considered responsible for them.

Appendix A. Supplementary data

Supplementary material related to this article can be found online at https://doi.org/10.1016/j.fusengdes.2024.114323.

References

[1] A. Molodyk, S. Samoilenkov, A. Markelov, P. Degtyarenko, S. Lee, V. Petrykin, M. Gaifullin, A. Mankevich, A. Vavilov, B. Sorbom, et al., Development and large volume production of extremely high current density YBa2Cu3O7 superconducting wires for fusion, Sci. Rep. 11 (1) (2021) 2084, http://dx.doi.org/10.1038/s41598-021-81559-z.

[2] L. Rossi, C. Senatore, HTS accelerator magnet and conductor development in europe, Instruments 5 (1) (2021) URL https://www.mdpi.com/2410-390X/5/1/8.

[3] E. Papadis, G. Tsatsaronis, Challenges in the decarbonization of the energy sector, Energy 205 (2020) 118025, http://dx.doi.org/10.1016/j.energy.2020.118025, URL https://www.sciencedirect.com/science/article/pii/S0360544220311324.

[4] S. Meschini, F. Laviano, F. Ledda, D. Pettinari, R. Testoni, D. Torsello, B. Panella, Review of commercial nuclear fusion projects, Front. Energy Res. 11 (2023) http://dx.doi.org/10.3389/fenrg.2023.1157394, URL https://www.frontiersin.org/articles/10.3389/fenrg.2023.1157394.

[5] B. Sorbom, J. Ball, T. Palmer, F. Mangiarotti, J. Sierchio, P. Bonoli, C. Kasten, D. Sutherland, H. Barnard, C. Haakonsen, et al., ARC: a compact, high-field, fusion nuclear science facility and demonstration power plant with demountable magnets, Fusion Eng. Des. 100 (2015) 378–405.

[6] C.G. Windsor, J.G. Morgan, Neutron and gamma flux distributions and their implications for radiation damage in the shielded superconducting core of a fusion power plant, Nucl. Fusion 57 (11) (2017) 116032, http://dx.doi.org/10.1088/1741-4326/aa7e3e.

[7] D. Torsello, D. Gambino, L. Gozzelino, A. Trotta, F. Laviano, Expected radiation environment and damage for YBCO tapes in compact fusion reactors, Supercond. Sci. Technol. 36 (1) (2022) 014003, http://dx.doi.org/10.1088/1361-6668/aca369.

[8] S. Segantin, R. Testoni, Z. Hartwig, D. Whyte, M. Zucchetti, Optimization of tritium breeding ratio in ARC reactor, Fusion Eng. Des. 154 (2020) 111531, http://dx.doi.org/10.1016/j.fusengdes.2020.111531, URL https://www.sciencedirect.com/science/article/pii/S092037962030079X.

[9] A.M. Sukegawa, K. Takiyoshi, T. Amano, H. Kawasaki, K. Okuno, Neutronic analysis of fusion tokamak devices by PHITS, Prog. Nucl. Sci. Technol. 1 (2011) 36–39.

[10] A. Kuang, N. Cao, A. Creely, C. Dennett, J. Hecla, B. LaBombard, R. Tinguely, E. Tolman, H. Hoffman, M. Major, J. Ruiz Ruiz, D. Brunner, P. Grover, C. Laughman, B. Sorbom, D. Whyte, Conceptual design study for heat exhaust management in the ARC fusion pilot plant, Fusion Eng. Des. 137 (2018) 221–242, http://dx.doi.org/10.1016/j.fusengdes.2018.09.007, URL https://www.sciencedirect.com/science/article/pii/S0920379618306185.

[11] T. Goorley, M. James, T. Booth, F. Brown, J. Bull, L.J. Cox, J. Durkee, J. Elson, M. Fensin, R.A. Forster, J. Hendricks, H.G. Hughes, R. Johns, B. Kiedrowski, R. Martz, S. Mashnik, G. McKinney, D. Pelowitz, R. Prael, J. Sweezy, L. Waters, T. Wilcox, T. Zukaitis, Initial MCNP6 release overview, Nucl. Technol. 180 (3) (2012) 298–315, http://dx.doi.org/10.13182/NT11-135.

[12] Y. Iwamoto, T. Sato, S. Hashimoto, T. Ogawa, T. Furuta, S. ichiro Abe, T. Kai, N. Matsuda, R. Hosoyamada, K. Niita, Benchmark study of the recent version of the PHITS code, J. Nucl. Sci. Technol. 54 (5) (2017) 617–635, http://dx.doi.org/10.1080/00223131.2017.1297742.

[13] P.K. Romano, B. Forget, The openmc Monte Carlo particle transport code, Ann. Nucl. Energy 51 (2013) 274–281, http://dx.doi.org/10.1016/j.anucene.2012.06.040, URL https://www.sciencedirect.com/science/article/pii/S0306454912003283.

[14] F. Tabbakh, Particles transportation and nuclear heating in a tokamak by MCNPX and GEANT4, J. Fusion Energy 35 (2) (2016) 401–406, http://dx.doi.org/10.1007/s10894-015-0047-9.

[15] J. Leppänen, M. Pusa, T. Viitanen, V. Valtavirta, T. Kaltiaisenaho, The serpent Monte Carlo code: Status, development and applications in 2013, Ann. Nucl. Energy 82 (2015) 142–150, http://dx.doi.org/10.1016/j.anucene.2014.08.024, Joint International Conference on Supercomputing in Nuclear Applications and Monte Carlo 2013, SNA + MC 2013. Pluri- and Trans-disciplinarity, Towards New Modeling and Numerical Simulation Paradigms. URL https://www.sciencedirect.com/science/article/pii/S0306454914004095.

[16] M. GOTO, N. NOJIRI, S. SHIMAKAWA, Neutronics calculations of HTTR with several nuclear data libraries, J. Nucl. Sci. Technol. 43 (10) (2006) 1237–1244, http://dx.doi.org/10.1080/18811248.2006.9711217, URL https://www.tandfonline.com/doi/abs/10.1080/18811248.2006.9711217.

[17] S. Aghara, S. Sriprisan, R. Singleterry, T. Sato, Shielding evaluation for solar particle events using MCNPX, PHITS and OLTARIS codes, Life Sci. Space Res. 4 (2015) 79–91, http://dx.doi.org/10.1016/j.lssr.2014.12.003, URL https://www.sciencedirect.com/science/article/pii/S2214552414000674.

[18] I. Meleshenkovskii, T. Ogawa, A. Sari, F. Carrel, K. Boudergui, Optimization of a 9 MeV electron accelerator bremsstrahlung flux for photofission-based assay techniques using PHITS and MCNP6 Monte Carlo codes, Nucl. Instrum. Methods Phys. Res. B 483 (2020) 5–14, http://dx.doi.org/10.1016/j.nimb.2020.10.002, URL https://www.sciencedirect.com/science/article/pii/S0168583X20304134.

[19] J.W. Bae, E. Peterson, J. Shimwell, ARC reactor neutronics multi-code validation*, Nucl. Fusion 62 (6) (2022) 066016, http://dx.doi.org/10.1088/1741-4326/ac5450.

[20] R. Juárez, R. Pampin, B. Levesy, F. Moro, A. Suarez, J. Sanz, Shutdown dose rates at ITER equatorial ports considering radiation cross-talk from torus cryopump lower port, Fusion Eng. Des. 100 (2015) 501–506, http://dx.doi.org/10.1016/j.fusengdes.2015.07.027, URL https://www.sciencedirect.com/science/article/pii/S0920379615302520.

[21] C. Yi-xue, W. Yi-can, Effect of fusion neutron source numerical models on neutron wall loading in a D-D tokamak device, Plasma Sci. Technol. 5 (2) (2003) 1749, http://dx.doi.org/10.1088/1009-0630/5/2/011.

[22] C. Fausser, A.L. Puma, F. Gabriel, R. Villari, Tokamak D-T neutron source models for different plasma physics confinement modes, Fusion Eng. Des. 87 (5) (2012) 787–792, http://dx.doi.org/10.1016/j.fusengdes.2012.02.025, Tenth International Symposium on Fusion Nuclear Technology (ISFNT-10). URL https://www.sciencedirect.com/science/article/pii/S0920379612000853.

[23] Y. Iwamoto, K. Niita, Y. Sakamoto, T. Sato, N. Matsuda, Validation of the event generator mode in the PHITS code and its application, in: International Conference on Nuclear Data for Science and Technology, EDP Sciences, 2007, pp. 945–948, http://dx.doi.org/10.1051/ndata:07417.

[24] Yang, Zi-Yi, Tsai, Pi-En, Lee, Shao-Chun, Liu, Yen-Chiang, Chen, Chin-Cheng, Sato, Tatsuhiko, Sheu, Rong-Jiun, Inter-comparison of dose distributions calculated by FLUKA, GEANT4, MCNP, and PHITS for proton therapy, EPJ Web Conf. 153 (2017) 04011, http://dx.doi.org/10.1051/epjconf/201715304011.

[25] M.C. Han, Y.S. Yeom, H.S. Lee, B. Shin, C.H. Kim, T. Furuta, Multi-threading performance of Geant4, MCNP6, and PHITS Monte Carlo codes for tetrahedral-mesh geometry, Phys. Med. Biol. 63 (9) (2018) 09NT02, http://dx.doi.org/10.1088/1361-6560/aabd20.

[26] Y.S. Yeom, M.C. Han, C. Choi, H. Han, B. Shin, T. Furuta, C.H. Kim, Computation speeds and memory requirements of mesh-type ICRP reference computational phantoms in Geant4, MCNP6, and PHITS, Health Phys. 116 (5) (2019) 664–676, http://dx.doi.org/10.1097/HP.0000000000000999.

[27] L. Sihver, D. Mancusi, K. Niita, T. Sato, L. Townsend, C. Farmer, L. Pinsky, A. Ferrari, F. Cerutti, I. Gomes, Benchmarking of calculated projectile fragmentation cross-sections using the 3-D, MC codes PHITS, FLUKA, HETC-HEDS, MCNPX-HI, and NUCFRG2, Acta Astronaut. 63 (7) (2008) 865–877, http://dx.doi.org/10.1016/j.actaastro.2008.02.012, From Dream to Reality: Living, Working and Creating for Humans in Space - A selection of papers presented at the 16th IAA Humans in Space Symposium, Beijing, China, 2007. URL https://www.sciencedirect.com/science/article/pii/S009457650800060X.

[28] A.M. Sukegawa, H. Kawasaki, K. Okuno, et al., Conceptual radiation shielding design of superconducting tokamak fusion device by PHITS, Prog. Nucl. Sci. Technol. 2 (2011) 375–381.

[29] P.K. Romano, N.E. Horelik, B.R. Herman, A.G. Nelson, B. Forget, K. Smith, Openmc: A state-of-the-art Monte Carlo code for research and development, Ann. Nucl. Energy 82 (2015) 90–97, http://dx.doi.org/10.1016/j.anucene.2014.07.048, Joint International Conference on Supercomputing in Nuclear Applications and Monte Carlo 2013, SNA + MC 2013. Pluri- and Trans-disciplinarity, Towards New Modeling and Numerical Simulation Paradigms. URL https://www.sciencedirect.com/science/article/pii/S030645491400379X.

[30] P. Shriwise, X. Zhang, A. Davis, DAG-openmc: CAD-based geometry in openmc, in: Proc. Amer. Nucl. Soc. Winter Meeting, Vol. 122, 2020, pp. 395–398.

[31] B. Mouginot, A. Davis, P. Shriwise, L. Jacobson, P. Wilson, M. Harb, K. Dunn, K. Kiesling, J. Shimwell, Z. Welch, N. Granda, J. Cary, M. Nyberg, X. Zhang, V. Mahadevan, h. brooks, P. Romano, E. Biondo, C. D'Angelo, N. Schlömer, M. Renken, I. Grindeanu, E. Xu, E. Relson, C. Perry, DAGMC - direct accelerated geometry Monte Carlo toolkit, 2021, URL https://github.com/svalinn/DAGMC.

[32] D.J. Kelly, B.N. Aviles, P.K. Romano, B.R. Herman, N.E. Horelik, B. Forget, Analysis of Select BEAVRS PWR Benchmark Cycle 1 Results Using MC21 and OpenMC, Tech. rep., IAEA, 2015.

[33] K.S. Chaudri, S.M. Mirza, Burnup dependent Monte Carlo neutron physics calculations of IAEA mtr benchmark, Prog. Nucl. Energy 81 (2015) 43–52, http://dx.doi.org/10.1016/j.pnucene.2014.12.018, URL https://www.sciencedirect.com/science/article/pii/S0149197015000037.

[34] T. Hu, L. Cao, H. Wu, X. Du, M. He, Coupled neutronics and thermal-hydraulics simulation of molten salt reactors based on OpenMC/TANSY, Ann. Nucl. Energy 109 (2017) 260–276, http://dx.doi.org/10.1016/j.anucene.2017.05.002, URL https://www.sciencedirect.com/science/article/pii/S0306454916309975.

[35] S. Segantin, S. Meschini, R. Testoni, M. Zucchetti, Preliminary investigation of neutron shielding compounds for ARC-class tokamaks, Fusion Eng. Des. 185 (2022) 113335, http://dx.doi.org/10.1016/j.fusengdes.2022.113335, URL https://www.sciencedirect.com/science/article/pii/S092037962200326X.

[36] T. Furuta, T. Sato, M.C. Han, Y.S. Yeom, C.H. Kim, J.L. Brown, W.E. Bolch, Implementation of tetrahedral-mesh geometry in Monte Carlo radiation transport code PHITS, Phys. Med. Biol. 62 (12) (2017) 4798, http://dx.doi.org/10.1088/1361-6560/aa6b45.

[37] J. Shimwell, P. Shriwise, Stl-to-5m: Convert non overlapping STL files into a DAGMC h5m file complete with material tags and ready for use in neutronics simulations. URL https://github.com/fusion-energy/stl_to_h5m.

[38] Openmc plasma source, 2021, Available on line. URL https://github.com/fusion-energy/openmc-plasma-source.

[39] K. SHIBATA, O. IWAMOTO, T. NAKAGAWA, N. IWAMOTO, A. ICHIHARA, S. KUNIEDA, S. CHIBA, K. FURUTAKA, N. OTUKA, T. OHSAWA, T. MURATA, H. MATSUNOBU, A. ZUKERAN, S. KAMADA, J. ichi KATAKURA, JENDL-4.0: A new library for nuclear science and engineering, J. Nucl. Sci. Technol. 48 (1) (2011) 1–30, http://dx.doi.org/10.1080/18811248.2011.9711675, arXiv:https://doi.org/10.1080/18811248.2011.9711675.

[40] D. Brown, M. Chadwick, R. Capote, A. Kahler, A. Trkov, M. Herman, A. Sonzogni, Y. Danon, A. Carlson, M. Dunn, D. Smith, G. Hale, G. Arbanas, R. Arcilla, C. Bates, B. Beck, B. Becker, F. Brown, R. Casperson, J. Conlin, D. Cullen, M.-A. Descalle, R. Firestone, T. Gaines, K. Guber, A. Hawari, J. Holmes, T. Johnson, T. Kawano, B. Kiedrowski, A. Koning, S. Kopecky, L. Leal, J. Lestone, C. Lubitz, J. Márquez Damián, C. Mattoon, E. McCutchan, S. Mughabghab, P. Navratil, D. Neudecker, G. Nobre, G. Noguere, M. Paris, M. Pigni, A. Plompen, B. Pritychenko, V. Pronyaev, D. Roubtsov, D. Rochman, P. Romano, P. Schillebeeckx, S. Simakov, M. Sin, I. Sirakov, B. Sleaford, V. Sobes, E. Soukhovitskii, I. Stetcu, P. Talou, I. Thompson, S. van der Marck, L. Welser-Sherrill, D. Wiarda, M. White, J. Wormald, R. Wright, M. Zerkle, G. Žerovnik, Y. Zhu, ENDF/B-VIII.0: the 8th major release of the nuclear reaction data library with CIELO-project cross sections, new standards and thermal scattering data, Nucl. Data Sheets 148 (2018) 1–142, http://dx.doi.org/10.1016/j.nds.2018.02.001, Special Issue on Nuclear Reaction Data. URL https://www.sciencedirect.com/science/article/pii/S0090375218300206.

[41] Evaluated nuclear data, 2021, Available on line. URL https://www.nndc.bnl.gov/endf-b8.0/.

[42] R. Forrest, R. Capote, N. Otsuka, T. Kawano, A. Koning, S. Kunieda, J.-C. Sublet, Y. Watanabe, FENDL-3 Library-Summary Documentation, Tech. rep., International Atomic Energy Agency, 2012.

[43] J.A. Kulesza, T.R. Adams, J.C. Armstrong, S.R. Bolding, F.B. Brown, J.S. Bull, T.P. Burke, A.R. Clark, R.A. Forster III, J.F. Giron, T.S. Grieve, C.J. Josey, R.L. Martz, G.W. McKinney, E.J. Pearson, M.E. Rising, C.J. Solomon Jr., S. Swaminarayan, T.J. Trahan, S.C. Wilson, A.J. Zukaitis, in: J.A. Kulesza (Ed.), MCNP® Code Version 6.3.0 Theory & User Manual, Tech. Rep. LA-UR-22-30006, Rev. 1, Los Alamos National Laboratory, Los Alamos, NM, USA, 2022, http://dx.doi.org/10.2172/1889957, URL https://www.osti.gov/biblio/1889957.

[44] A. Aimetta, N. Abrate, S. Dulla, A. Froio, Neutronic analysis of the fusion reactor ARC: Monte Carlo simulations with the serpent code, Fusion Sci. Technol. 78 (4) (2022) 275–290, http://dx.doi.org/10.1080/15361055.2021.2003151.
[45] See Supplemental Material at https://doi.org/10.1016/j.fusengdes.2024.114323 which includes further details on the materials compositions, computational times and power deposition.
[46] openmc-dev/data, Available online. URL https://github.com/openmc-dev/data.
[47] openmc-data-storage/openmc_dataF, Available online. URL https://github.com/openmc-data-storage/openmc_data.
[48] hpc4, Available online. URL https://www.eni.com/en-IT/media/press-release/2018/01/eni-boots-up-hpc4-and-makes-its-computing-system-the-worlds-most-powerful-in-the-industry.html.